

We are IntechOpen, the world's leading publisher of Open Access books Built by scientists, for scientists

6,900

Open access books available

186,000

International authors and editors

200M

Downloads

Our authors are among the

154

Countries delivered to

TOP 1%

most cited scientists

12.2%

Contributors from top 500 universities



WEB OF SCIENCE™

Selection of our books indexed in the Book Citation Index
in Web of Science™ Core Collection (BKCI)

Interested in publishing with us?
Contact book.department@intechopen.com

Numbers displayed above are based on latest data collected.
For more information visit www.intechopen.com



Air Pollution Monitoring Using Earth Observation & GIS

Diofantos G. Hadjimitsis, Kyriacos Themistocleous and Argyro Nisantzi
*Cyprus University of Technology
Cyprus*

1. Introduction

Air pollution has received considerable attention by local and global communities (Wald et al, 1999). Many major cities have established air quality monitoring stations but these stations tend to be scarcely distributed and do not provide sufficient tools for mapping atmospheric pollution since air quality is highly variable (Wald et al, 1999). Satellite remote sensing is a valuable tool for assessing and mapping air pollution as satellite images are able to provide synoptic views of large areas in one image on a systematic basis due to the temporal resolution of the satellite sensors. Blending together earth observation with ground supporting campaigns enables the users or governmental authorities to validate air pollution measurements from space. New state-of-the-art ground systems are used to undertake field measurements such as Lidar system, automatic and hand held sun-photometers etc. The rise of GIS technology and its use in a wide range of disciplines enables air quality modellers with a powerful tool for developing new analysis capability. Indeed, thematic air pollution maps can be developed. Moreover, the organization of data by location allows data from a variety of sources to be easily combined in a uniform framework. GIS provides the opportunity to fill the technical gap between the need of analysts and decision-makers for easy understanding of the information.

This Chapter presents an overview of how earth observation basically is used to monitor air pollution through an overview of the existing ground and space systems as well through the presentation of several case studies.

2. Relevant literature review

The use of earth observation to monitor air pollution in different geographical areas and especially in cities has received considerable attention (Kaufman and Fraser, 1983; Kaufman et al., 1990; Sifakis and Deschamps, 1992; Retalis, 1998; Retalis et al., 1998; Sifakis et al., 1998; Retalis et al., 1999; Wald and Balleynaud, 1999; Wald et al., 1999; Hadjimitsis et al., 2002; Themistocleous et al., 2010; Nisantzi et al. 2011; Hadjimitsis et al., 2011). All the studies have involved the determination of aerosol optical thickness (AOT) either using indirect methods using Landsat TM/ETM+, ASTER, SPOT, ALOS, IRS etc. images or MODIS images in which AOT is given directly. The superior spatial resolution of Landsat and SPOT enable several researchers to develop a variety of methods based on the radiative transfer equation,

atmospheric models and image-based methods. Indeed, Kaufman et al. (1990) developed an algorithm for determining the aerosol optical thickness (using land and water dark targets) from the difference in the upward radiance recorded by the satellite between a clear and a hazy day. This method assumes that the surface reflectance between the clear day and the hazy day images does not change. Sifakis and Deschamps (1992) used SPOT images to estimate the distribution of air pollution in the city of Toulouse in France. Sifakis and Deschamps (1992) developed an equation to calculate the aerosol optical depth difference between one reference image (acquired under clear atmospheric conditions) and a polluted image. Their method was based on the fact that, after correction of solar and observation angle variations, the remaining deviation of apparent radiances is due to pollutants. Retalis (1998) and Retalis et al. (1999) showed that an assessment of the air pollution in Athens could be achieved using the Landsat TM band 1 by correlating the aerosol optical thickness with the acquired air-pollutants. Moreover, Hadjimitsis and Clayton (2009) developed a method that combines the Darkest Object Subtraction (DOS) principle and the radiative transfer equations for finding the AOT value for Landsat TM bands 1 and 2. Hadjimitsis (2009a) used a new method for determining AOT through the use of the darkest pixel atmospheric correction over the London Heathrow Airport area in the UK and the Pafos Airport area in Cyprus. Hadjimitsis (2009b) developed a method to determine the aerosol optical thickness through the application of the contrast tool (maximum contrast value), the radiative transfer calculations and the 'tracking' of the suitable darkest pixel in the scene for Landsat, SPOT and high resolution imagery such as IKONOS and Quickbird.

Satellite remote sensing is certainly a valuable tool for assessing and mapping air pollution due to their major benefit of providing complete and synoptic views of large areas in one image on a systematic basis due to the good temporal resolution of various satellite sensors (Hadjimitsis et al., 2002). Chu et al. (2002) and Tang et al. (2004) reported that the accuracy of satellite-derived AOT is frequently assessed by comparing satellite based AOT with AERONET (Aerosol RObotic NETwork - a network of ground-based sun-photometers) or field based sun-photometer. The determination of the AOT from the Landsat TM/ETM+ imagery is based on the use of radiative transfer equation, the principle of atmospheric correction such as darkest pixel method (Hadjimitsis et al., 2002). Since MODIS has a sensor with the ability to measure the total solar radiance scattered by the atmosphere as well as the sunlight reflected by the Earth's surface and attenuated by atmospheric transmission, the AOT results found by MODIS were compared with the sun-photometer's AOT results for systematic validation (Tang et al., 2004). For the MODIS images, despite its low pixel resolution, aerosol optical thickness values were extracted for the 550 nm band. MODIS data have been extended correlated with PM10 over several study areas (Hadjimitsis et al., 2010; Nisanzi et al., 2011) with improved correlation coefficients but with several limitations. PM2.5 are also found to be correlated against MODIS data using new novel improved algorithms (e.g Lee et al., 2011) that considers the low spatial resolution of MODIS with future positive premises. Themistocleous et al. (2010) used Landsat TM/ETM+ and MODIS AOT data to investigate the air pollution near to cultural heritage sites in the centre of Limassol area in Cyprus. Nisanzi et al. (2011) used both particulate matter (PM10) device, backscattering lidar system, AERONET and hand-held sun-photometers for developing PM10 Vs MODIS AOT regression model over the urban area of Limassol in Cyprus.

It is expected that future satellite technologies will provide data with finer spatial and temporal resolutions and more accurate data retrievals (Lee et al., 2011). Moreover, the advanced capability of discriminating by aerosol species in satellite technologies will further contribute to health effect studies investigating species-specific health implications (Lee et al., 2011).

3. Aerosol Optical Thickness – Aerosol Optical Depth (AOD)

The key parameter for assessing atmospheric pollution in air pollution studies is the aerosol optical thickness, which is also the most important unknown element of every atmospheric correction algorithm for solving the radiative transfer equation and removing atmospheric effects from satellite remotely sensed images (Hadjimitsis et al, 2004). Aerosol optical thickness (AOT) is a measure of aerosol loading in the atmosphere (Retalis et al, 2010). High AOT values suggest high concentration of aerosols, and therefore air pollution (Retalis et al, 2010). The use of earth observation is based on the monitoring and determination of AOT either direct or indirect as tool for assessing and measure air pollution. Measurements on PM10 and PM2.5 are found to be related with the AOT values as shown by Lee et al. (2011), Hadjimitsis et al. (2010), Nisantzi et al. (2011).

"Aerosol Optical Thickness" is defined as the degree to which aerosols prevent the transmission of light. The aerosol optical depth or optical thickness (τ) is defined as 'the integrated extinction coefficient over a vertical column of unit cross section. Extinction coefficient is the fractional depletion of radiance per unit path length (also called attenuation especially in reference to radar frequencies)'. (http://daac.gsfc.nasa.gov/data-holdings/PIP/aerosol_optical_thickness_or_depth.shtml).

4. PM10

Particulate matter (PM10) pollution consists of very small liquid and solid particles floating in the air. PM10 particles are less than 10 microns in diameter. This includes fine particulate matter known as PM2.5. PM10 is a major component of air pollution that threatens both our health and our environment.

5. Satellite imagery

Several remotely sensed data are used to provide direct or indirect air or atmospheric pollution measurements. MODIS satellite imagery provides direct AOT measurements; however, Landsat TM/ETM+, ASTER, SPOT or other satellites provide indirect measurements of AOT through the application of specific techniques.

5.1 MODIS

The Moderate Resolution Imaging Spectroradiometer (MODIS) onboard NASA's Terra spacecraft performs near-global daily observations of atmospheric aerosols. The MODIS instrument measures upwelling radiance in 36 bands for wavelengths ranging from 0.4 to 14.385 μm and has a spatial resolution of 250m (2 channels), 500m (5 channels), and 1 km (29 channels) at nadir. (Kaufman et al, 1997; Tanré et al, 1997, 1999; Remer et al, 2005 ; Vermote and Saleous, 2000). The aerosol retrieval makes use of 7 of these channels (0.47 – 2.12 μm) to

retrieve aerosol boundaries and characteristics. MODIS has one camera and measures radiances in 36 spectra bands, from 0.4 μm to 14.5 μm with spatial resolutions of 250m (bands 1-2), 500 m (bands 3-7) and 1000 m (bands 8-36). Daily level 2 (MOD04) aerosol optical thickness data (550 m) are produced at the spatial resolution of 10x10 km over land, using the 1 km x 1 km cloud-free pixel size. MODIS aerosol products are provided over land and water surfaces. Typical MODIS satellite image with raw AOT values over Cyprus is shown in Figure 1.

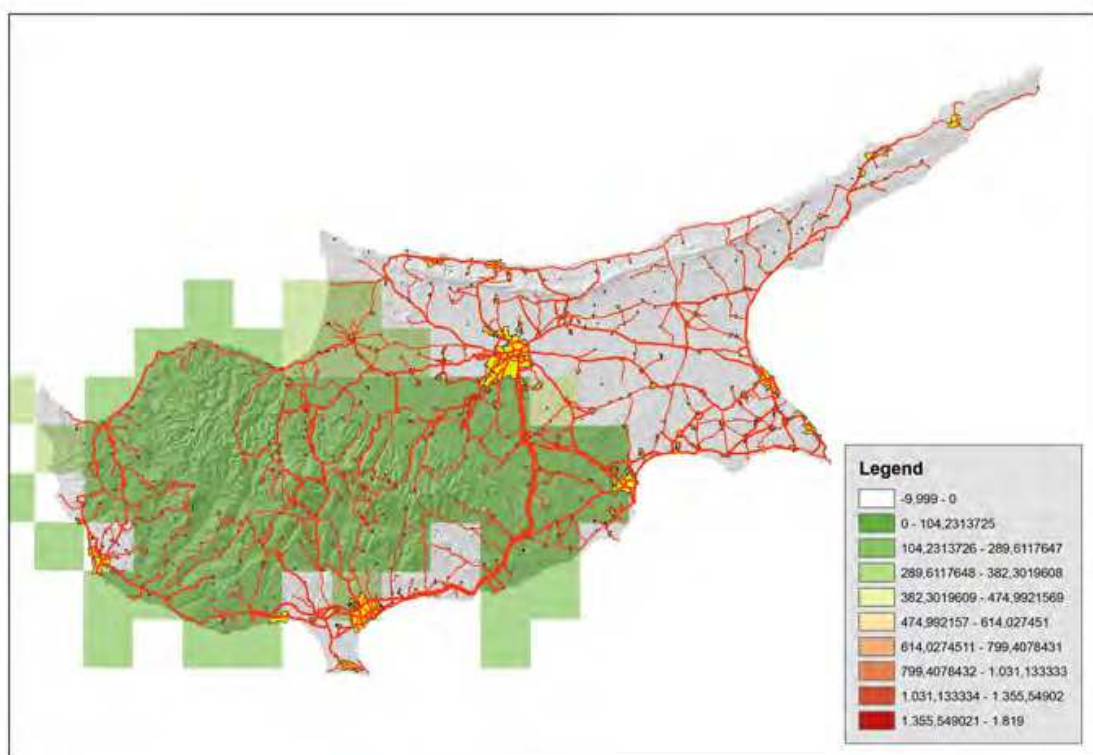


Fig. 1. MODIS AOT satellite image (direct measurements of AOT).

5.2 ASTER

ASTER is an advanced multi-spectral imager that was launched onboard NASA's Terra spacecraft in December 1999. ASTER covers a wide spectral region with 14 bands from visible to thermal infrared with high spatial, spectral and radiometric resolutions. The spatial resolution varies with wavelength: 15m in the visible and near-infrared (VNIR), 30m in the short wave infrared (SWIR), and 90m in the thermal infrared (TIR).

5.3 LANDSAT TM/ETM+

The Landsat Thematic Mapper (TM) is an advanced, multi-spectral scanning, Earth resources sensor designed to achieve higher spatial resolution, sharper spectral separation, improved geometric fidelity, and greater radiometric accuracy and resolution (Guanter, 2006). TM data are scanned simultaneously in 7 spectral bands. Band 6 scans thermal (heat) infrared radiation, the other ones scan in the visible and infrared. The Enhanced Thematic Mapper-Plus (ETM+) on Landsat-7 that was launched on April 15, 1999 is providing observations at a higher spatial resolution and with greater measurement precision than the previous TM

6. Ground measurements for supporting remote sensing measurements

As both direct or indirect retrieval of the aerosol optical thickness from satellites require ground validation, several resources (equipments, systems) are available to support such outcomes. The authors provide an overview of the existing systems which are used to support the air pollution measurements from space. Such systems are available at the Cyprus University of Technology-The Remote Sensing Laboratory.

6.1 Automatic sun-photometer (AERONET)

The CIMEL sun-tracking photometer (Fig.2) measures sun and sky luminance in visible and near-infrared. Specifically, it measures the direct solar radiance at 8 wavelengths (340nm, 380nm, 440nm, 500nm, 675nm, 870nm, 1020nm, 1640nm) and sky radiance at four of these wavelengths (440nm, 670nm, 865nm, 1020nm) providing information for determination of aerosol optical properties such as size distribution, angstrom exponent, refractive index, phase function and AOT. The CIMEL sun-photometer is calibrated according to program of AERONET specifications. An example of how measurements of AERONET aerosol optical depth (AOD) retrievals compared with the AOD derived from satellite MODIS data are correlated are shown in Figure 3. Such regression models are essential in order to test and validate the AOD retrieved from satellites with ground measurements.



Fig. 2. CIMEL sun-photometer (Cyprus University of Technology Premises: Remote Sensing Lab).

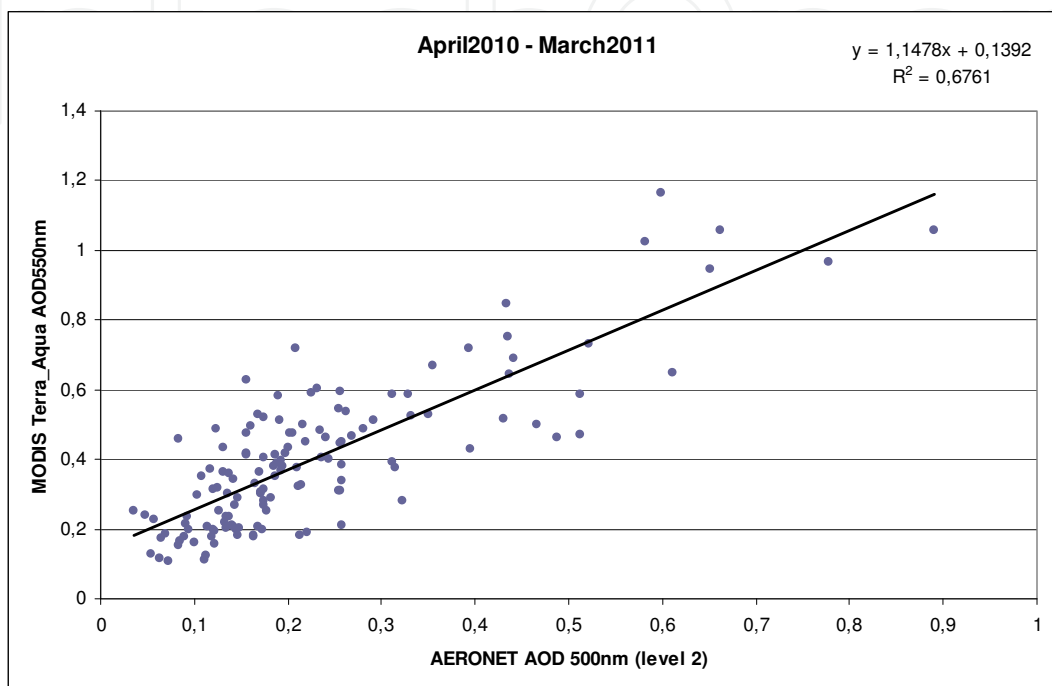


Fig. 3. Correlation between MODIS AOD and AERONET AOD (level 2) for Limassol, April 2010 - March 2011.

6.2 Hand-held sun-photometer

The MICROTUPS II is a hand-held multi-band sun photometer (fig. 4). The sun-photometer measures the aerosol optical thickness (440 nm, 675 nm, 870 nm, 936 nm and 1020 nm bands) and precipitable water (936nm and 1020nm bands) through the intensity of direct sunlight. The sun-photometer consists of five optical collimators (field of view 2.5 degrees) while the internal baffles eliminate the reflections occurred within the instrument. In order to extract the aerosol optical thickness the Langley method was used.

Such hand-held sun-photometers are useful to assess the effectiveness of the AOT measurements derived from satellites. For example, Figure 5 shows the results obtained from applying a linear regression model concerning the satellite AOT retrievals and ground-based Microtops derived AOT for more than two years measurements in the area of Limassol centre area in Cyprus.



Fig. 4. View of hand-held sun photometer (MICROTOPS II sun-photometer).

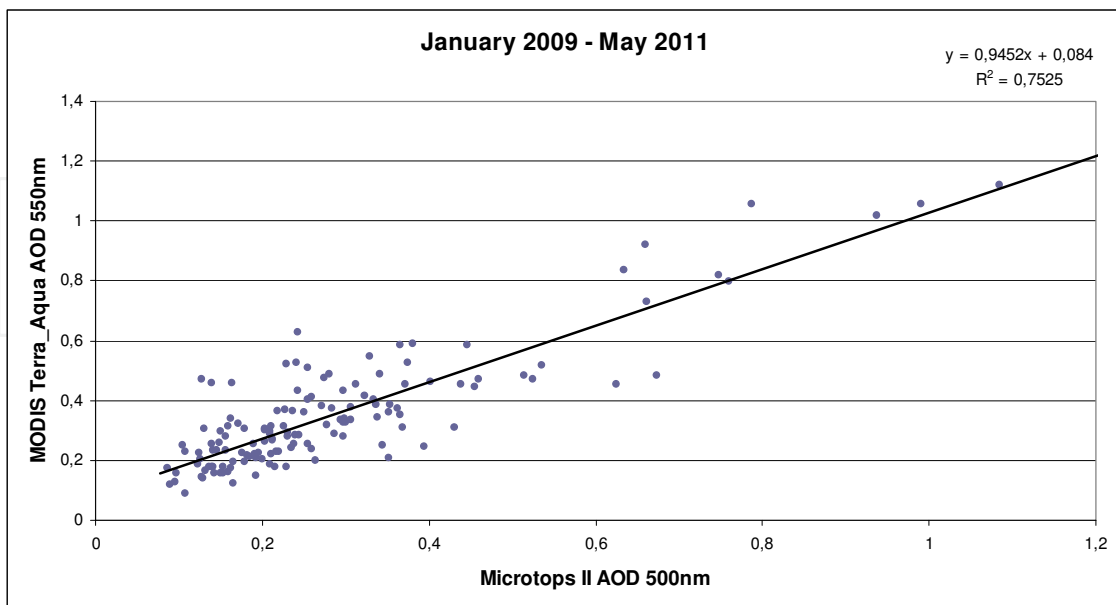


Fig. 5. Correlation between MODIS and Microtops AOD for Limassol, January 2009 - May 2011.

6.3 LIDAR

The Lidar system (see Fig.6) is able to provide aerosol or cloud backscatter measurements from a height beginning from 200m up to tropopause height. The Lidar emits a collimated laser beam in the atmosphere and then detects the backscattered laser light from atmospheric aerosols and molecules. The Lidar transmits laser pulses at 532 and 1064 nm simultaneously and co-linearly with a repetition rate of 20 Hz. Three channels are detected, with one channel for the wavelength 1064 nm and two channels for 532 nm. One small, rugged, flash lamp-pumped Nd-YAG laser is used with pulse energies around 25 and 56 mJ at 1064 and 532 nm, respectively. The primary mirror has an effective diameter of 200 mm. The overall focal length of the telescope is 1000 mm. The field of view (FOV) of the telescope is 2 mrad.



Fig. 6. Light Detection and Ranging, Lidar System.

Using the two different wavelength of lidar we can extract aerosol optical properties such as color index (CI), aerosol backscatter and extinction coefficient, Angstrom exponent, depolarization ratio and AOT, which are all useful parameters for characterizing the type and the shape of particles within the atmosphere. Moreover the lidar system can be used for the detection of clouds and the provision of the Planetary Boundary Layer (PBL) height in near-real time. The data that was extracted after the processing of lidar signals is shown in Fig. 7 and 8. Such data are important for supporting the findings from satellite imagery and through systematic measurements a local atmospheric model can be used for future applications. Moreover, air pollution episodes can be fully supported and explained. According to Fig. 7 and 7, the PBL extends from the surface up to 1600m and there are also two layers above the PBL, the first are centred around 3300m and the second at 3800m. Additionally there are multiple layers within the PBL and it can be distinguished not only by the different colours of temporal evolution of atmosphere (fig.7) but from the peaks presents in the signal of backscatter coefficient (fig.8).

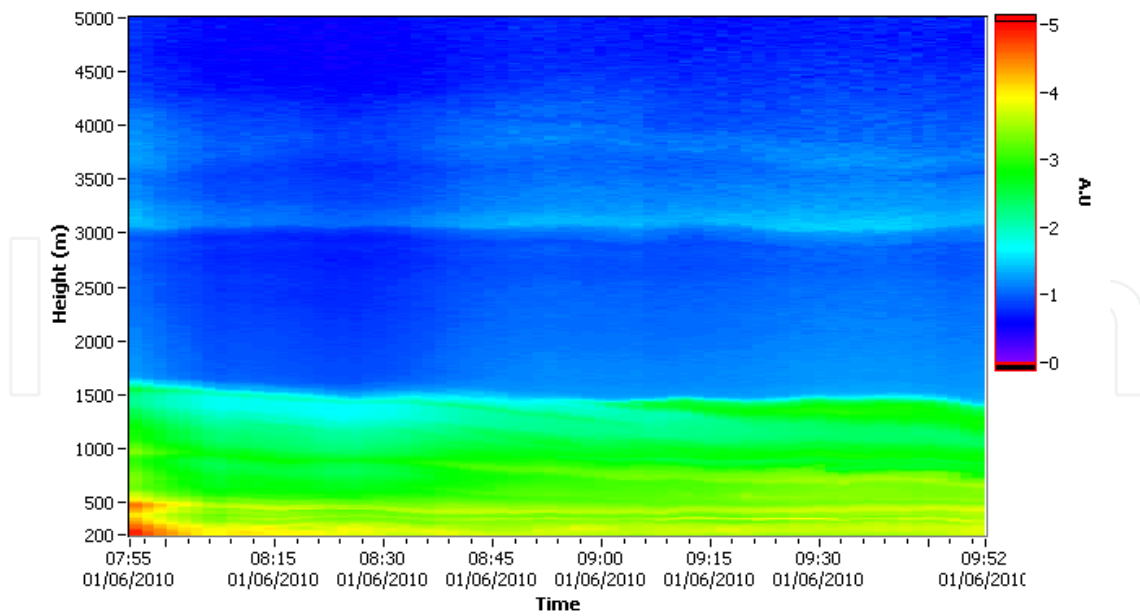


Fig. 7. Temporal evolution of the dust layers over Limassol on 1st of June 2010: Profile from the Lidar system.

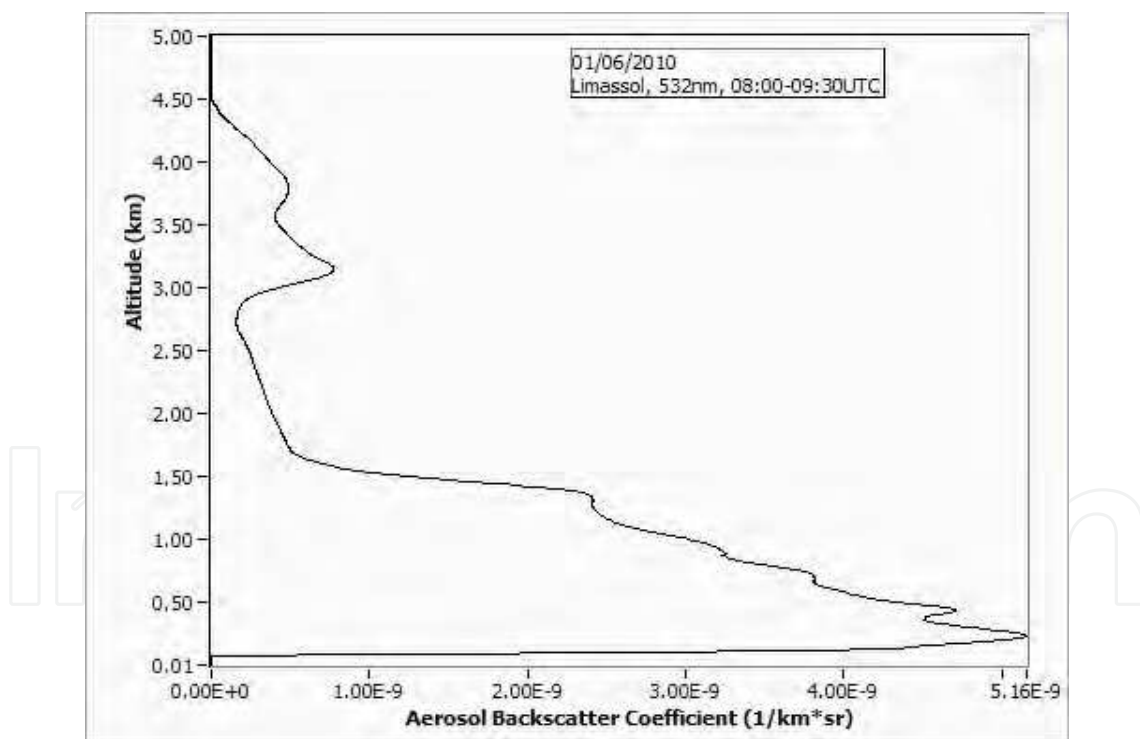


Fig. 8. The vertical distribution of the backscatter coefficient on 1 June 2010, Limassol.

6.4 PM10 device

Several PM10 devices are available to measure particulate matter. Such devices can be used to develop regression models between PM10 measurements with AOT values obtained from satellites, which assists in the systematic monitoring of PM10 from space.

For example, the TSI DustTrak (model 8520/ 8533) (fig. 9) is a light scattering laser photometer that is used to measure PM mass concentrations. The instrument specifically measures the amount of scattering light which is proportional to volume concentrations of aerosols and it could obtain the mass concentration of them. The instrument is placed in the Environmental Enclosure and is mounted to a standard surveyor tripod for allowing reliable and accurate sampling.



Fig. 9. PM10 devices (for example, Dust Trak model 8533/ 8520).

6.5 Field spectroradiometers

Several spectroradiometers are available to support the effective removal of atmospheric effects from satellite imagery such as the GER-1500 and SVC HR-1024 field spectroradiometers (see Fig.10). Spectroradiometers are used to retrieve the ground reflectance of various standard calibration targets. The GER1500 field spectroradiometer are light-weight, high performance covering the visible and near-infrared wavelengths from 350 nm to 1050 nm while the SVC HR-1024 provides high resolution field measurements between 350 nm and 2500 nm. The application of an effective atmospheric correction algorithm by using the retrieved ground reflectance values in conjunction with the use of the radiative transfer equation provides an indirect method for determining the aerosol optical thickness. Field spectroradiometric measurements are acquired over dark targets such as asphalt areas (see Fig.10) so as to retrieve the AOT values through the application of atmospheric correction algorithms over satellite imagery such as Landsat TM/ETM+, ASTER, SPOT, ALOS, IRS etc.



Fig. 10. Field spectroradiometric measurements over dark asphalt target.

7. Case studies

7.1 Case study 1: Retrieval of aot through the application of rt equation and atmospheric correction algorithm

Hadjimitsis et al. (2010) provides several examples of how Lidar and sun-photometers measurements can support the AOT values found from the Landsat TM/ETM+ satellite images. AOT values are derived from Landsat TM/ETM+ images using the darkest pixel atmospheric correction method and radiative transfer equation.

The basic equations used to retrieve AOT values is described by Hadjimitsis and Clayton (2009) has been fully applied. The revised method presented by Hadjimitsis et al. (2010) differs from the traditional DOS (Darkest Object Subtraction) method in the following ways: The method incorporates the true reflectance value which is acquired from in-situ spectroradiometric measurements of selected pseudo-invariant dark-targets such as dark water bodies or asphalt black surfaces (fig.9); the method combines both the basic principles of the darkest object subtraction and radiative transfer equations by incorporating in the calculations the aerosol single scattering phase function, single scattering albedo and water vapour absorption (i.e. Relative Humidity) (values as acquired from several in-situ measurements).

The retrieved target reflectance is given by equation 1:

$$\rho_{tg} = \frac{\pi \cdot (L_{ts} - L_p)}{t(\mu) \uparrow \cdot E_G} \quad (1)$$

where

ρ_{tg} is the target reflectance at ground level

L_{ts} is the at-satellite radiance (integrated band radiance measured in W/m²/sr)

L_p is the atmospheric path radiance (integrated band radiance measured in W/m²/sr)

E_G is the global irradiance reaching the ground

$t(\mu) \uparrow$ is the direct (upward) target-sensor atmospheric transmittance

For a dark object such as a large water reservoir the target reflectance (at ground level, $\rho_{tg} = \rho_{dg}$) is very low but is not zero. From this large reservoir the darkest pixel will be seen at-satellite to have radiance $L_{ts} = L_{ds}$. Therefore equation 1 can be re-written as:

$$\rho_{dg} = \frac{\pi \cdot (L_{ds} - L_p)}{t(\mu) \uparrow \cdot E_G} \quad (2)$$

where

ρ_{dg} is the dark target reflectance at ground level

L_{ds} is the dark target radiance at the sensor in W/m²/sr

The aerosol optical thickness was calculated using equation 3 as given by Hadjimitsis and Clayton (2009) [3]:

$$L_{pa} = \omega_a \left\{ \frac{(E_G \cdot \cos(\theta_0) \cdot P_a)}{4\pi(\cos(\theta_0) + \cos(\theta_v))} \right\} \cdot \left\{ 1 - \exp[-\tau_a(1/\cos\theta_0 + 1/\cos\theta_v)] \right\} \cdot t_{H_2O} \uparrow \cdot t_{O_3} \uparrow \cdot \exp[-\tau_r(1/\cos\theta_0 + 1/\cos\theta_v)] \quad (3)$$

The algorithm as presented by Hadjimitsis and Clayton (2009) required the following parameters:

- ground reflectance values for the selected ground dark target either zero or any value up to 5 % until the AOT value gets maximum (from spectro-radiometric measurements, suitable water target, for example for water dams values of 0 to 5 % for TM band 1)
- the at-satellite reflectance value of the darkest pixel or target (from the image)
- and the aerosol characteristics (e.g. aerosol scattering albedo) unless you will make assumptions based on previous studies .eg for urban areas aerosol scattering albedo=0.78

By running equation (3) and (2), AOT value was found for Landsat TM band 1.

The first example indicates the AOT values as measured by CIMEL sun-photometer for the whole day, 20/4/2010 as well for the whole month (see Figures 10 and 11). For the Landsat ETM+ image acquired on 20/4/2010, the AOT was found to be 1.4 after the application of the darkest pixel atmospheric correction i.e indirect method of retrieving AOT values. Such value complies with the AOT value found during the satellite overpass for that day as shown from Figure 11. Figure 12 shows that the daily AOT values for April 2010 from AERONET, the 20th of April 2010 has the highest value.

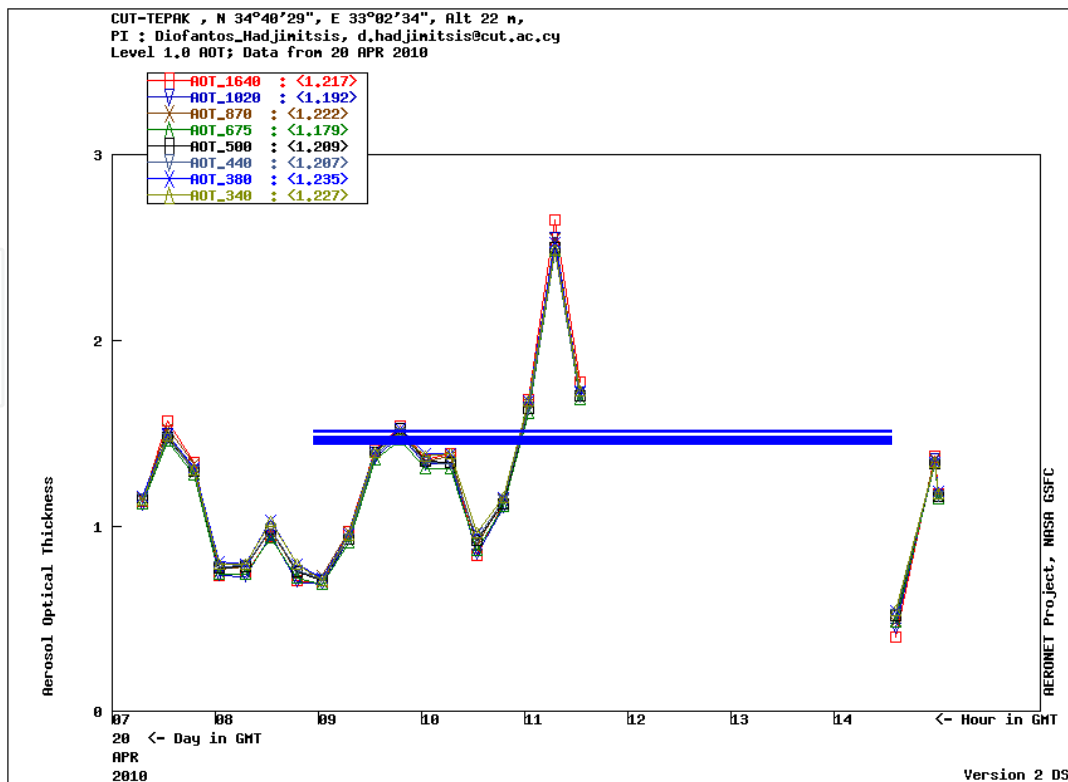


Fig. 11. Daily distribution of AOT by AERONET for the 20th of April 2010. (Hadjimitsis et al., 2010).

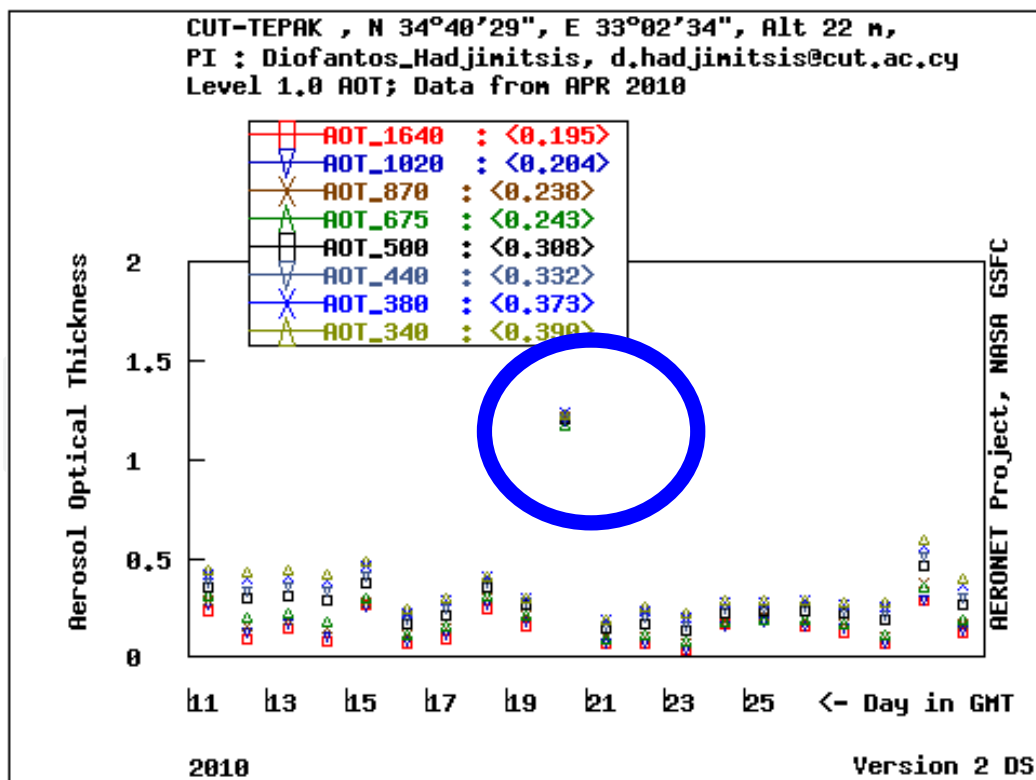


Fig. 12. Monthly distribution of AOT (11-30/ April/2010) by AERONET (Hadjimitsis et al., 2010).

Hadjimitsis et al. (2010) provided another example for the May 2010 (27th and 28th of May 2010) measurements both from LIDAR and AERONET. An assessment of the existing atmospheric conditions was done using Lidar system and CIMEL sun-photometers for the 27th and 28th of May 2010 in which dust scenarios were occurred. By considering the values given by the CIMEL sun-photometer as well the support given by the Lidar regarding the dust event, the user assessed air pollution through the application of the atmospheric correction algorithm. By using three months of measurements with both CIMEL sun-photometer and LIDAR, it was found that the mean daily value of Aerosol Optical Thickness exceeded 0.7, while the highest value of AOT during the day was 1.539 (Figure 13).

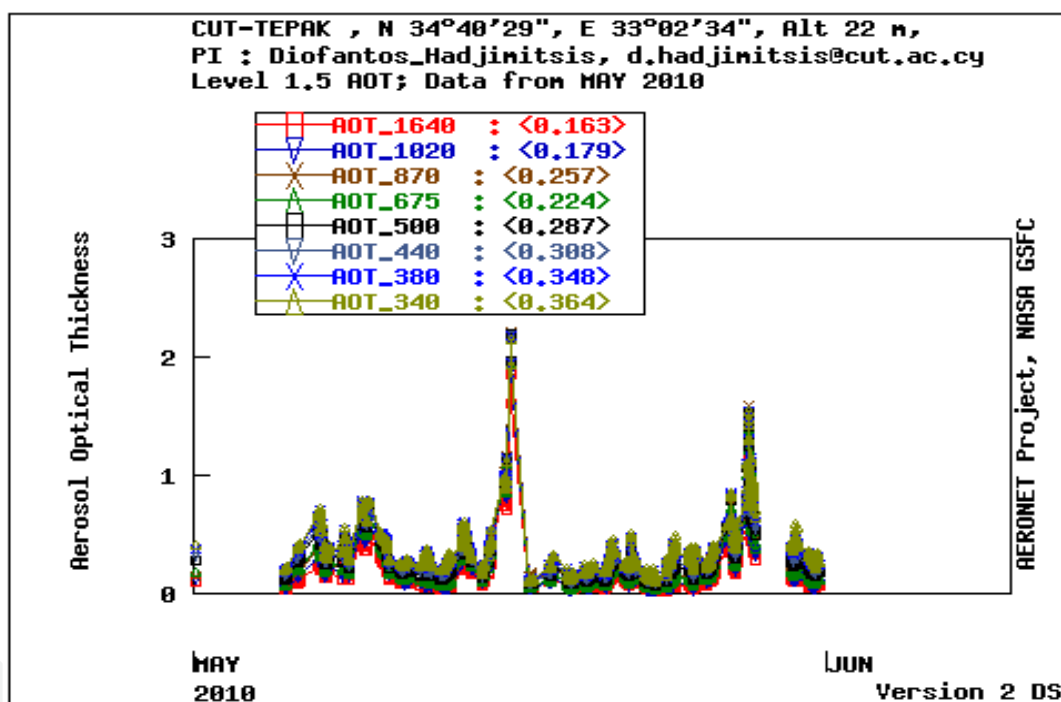
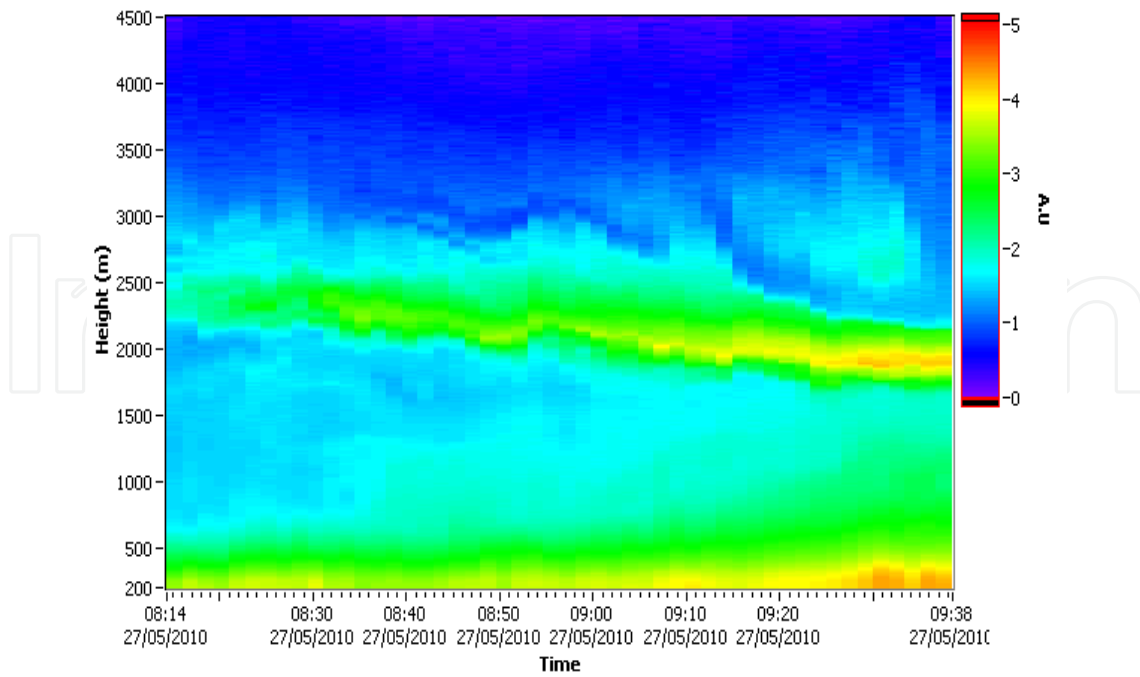
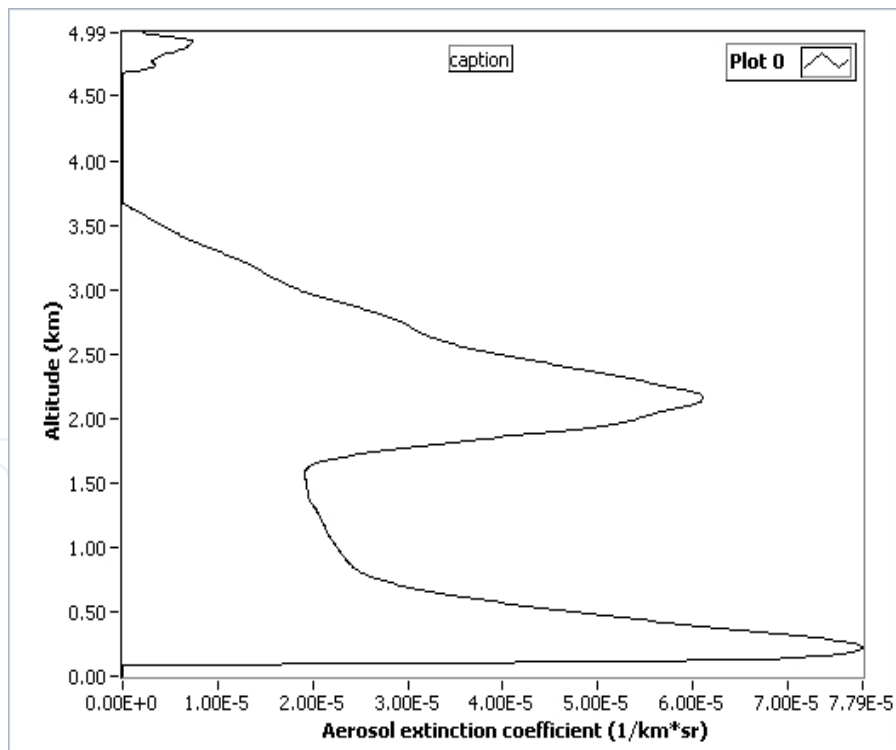


Fig. 13. Monthly distribution of AOT (May) by AERONET (Hadjimitsis et al., 2010).

The measurements from LIDAR showed the previous day a distinct layer in a height between 2 and 3 km (Fig.14). Thus the dust layer in a specific altitude above the Planetary Boundary Layer (PBL) followed the high AOT values a day after as prescribed the CIMEL sun-photometer from AERONET. Moreover, according to Hadjimitsis et al. (2010), in order to verify dust transport to Cyprus, the NOAA Hysplit Model was used, which provided three-days air-mass back-trajectories in three different levels within the atmosphere. The relevant 72-h back-trajectory analysis for air-masses ending over Limassol, Cyprus at 00:00 UT on 28 May is presented in Figure 15. It is remarkable that for 28 May all air-mass trajectories ending over Limassol at levels between 1km and 4km originated from Saharan at levels 0.5-4 km.



(a)



(b)

Fig. 14. (a) Temporal evolution of a dust layer at an altitude of 1.9-2.6 km over the area of Limassol (b) vertical distribution of the aerosol extinction coefficient in a case of high aerosol loading (27/05/2010) (Hadjimitsis et al., 2010).

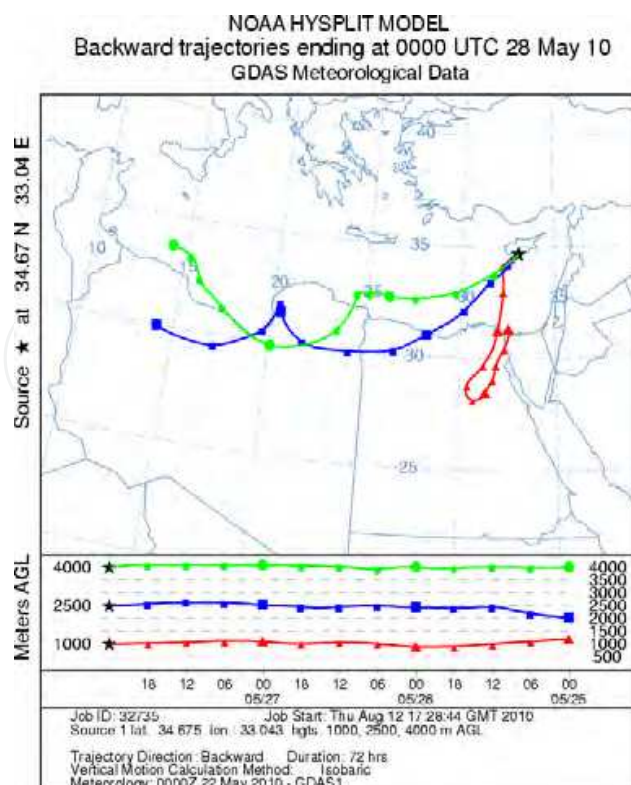


Fig. 15. 72-h air-mass back-trajectories ending over Limassol, Cyprus at 00:00 UT on 28 May 2010 (Hadjimitsis et al., 2010).

By extending the same procedure over a large area of interest, AOT maps can be produced using Landsat TM/ETM+ imagery as shown in Fig. 16



Fig. 16. AOT map from Landsat TM images using indirect method such as the application of atmospheric correction (Themistocleous et al., 2010).

7.2 Case study 2: Retrieval of aot from modis and development of regression model between aot vs pm10

Nisantzi et al. (2011) show how MODIS AOT data can be correlated with PM10 over an urban area in Limassol, Cyprus. Based on the developed regression models, such model can be used for systematic monitoring of air pollution such as PM10 over the urban area of Limassol. Nisantzi et al. (2011) made a comparison between MODIS AOD at 550nm and AERONET AOD (automatic-sun photometer as shown in Fig.2). The number of measurements are 136 and the correlation coefficient according to coefficient of determination ($R^2 = 0.67$) is $R=0.822$ (fig.16). These results indicate that MODIS-derived AOD values can be used in case of no AERONET AOD will be available and vice versa. Similarly MODIS AOD compared with Microtops II (See Fig.3) AOD at 500nm and the retrievals for 141 data shows a better correlation $R=0.867$ ($R^2=0.7525$) for more than two years measurements (fig.18).

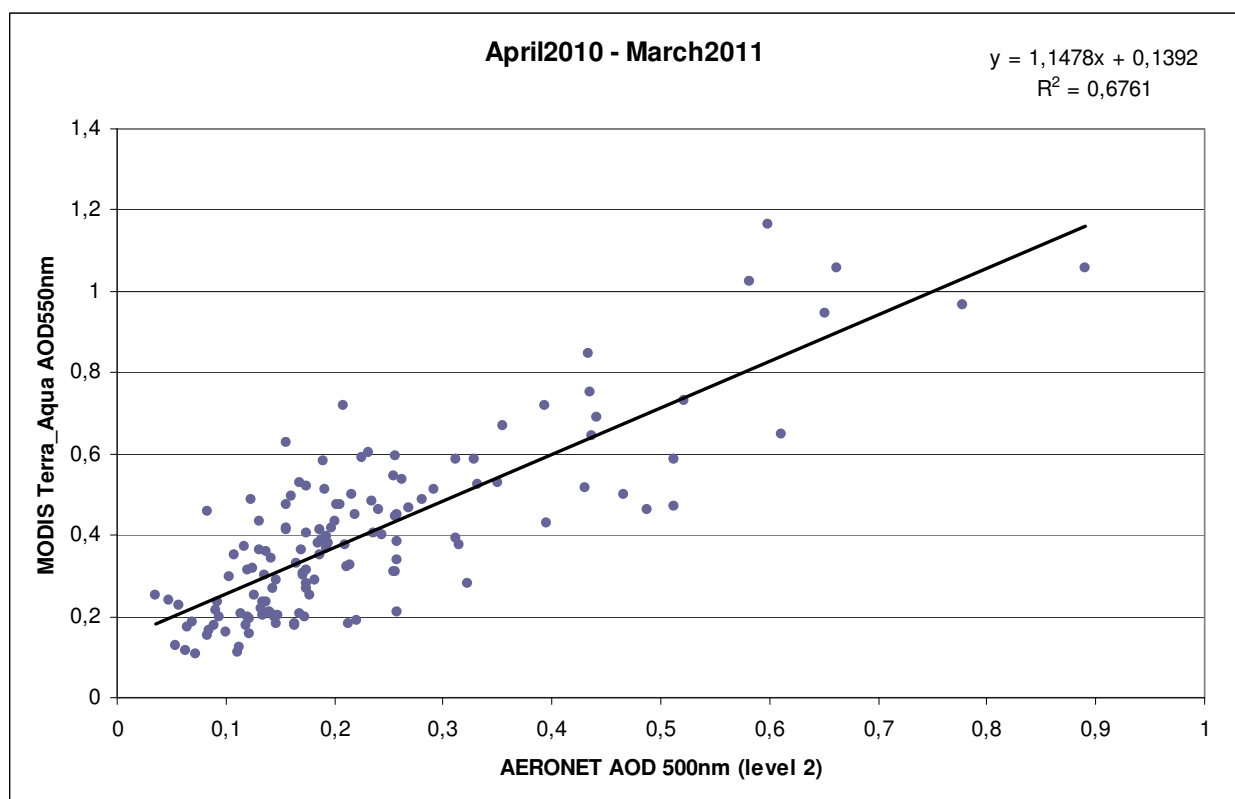


Fig. 17. Correlation between MODIS AOD and AERONET AOD (level 2) for Limassol, April 2010 - March 2011. (Nisantzi et al., 2011).

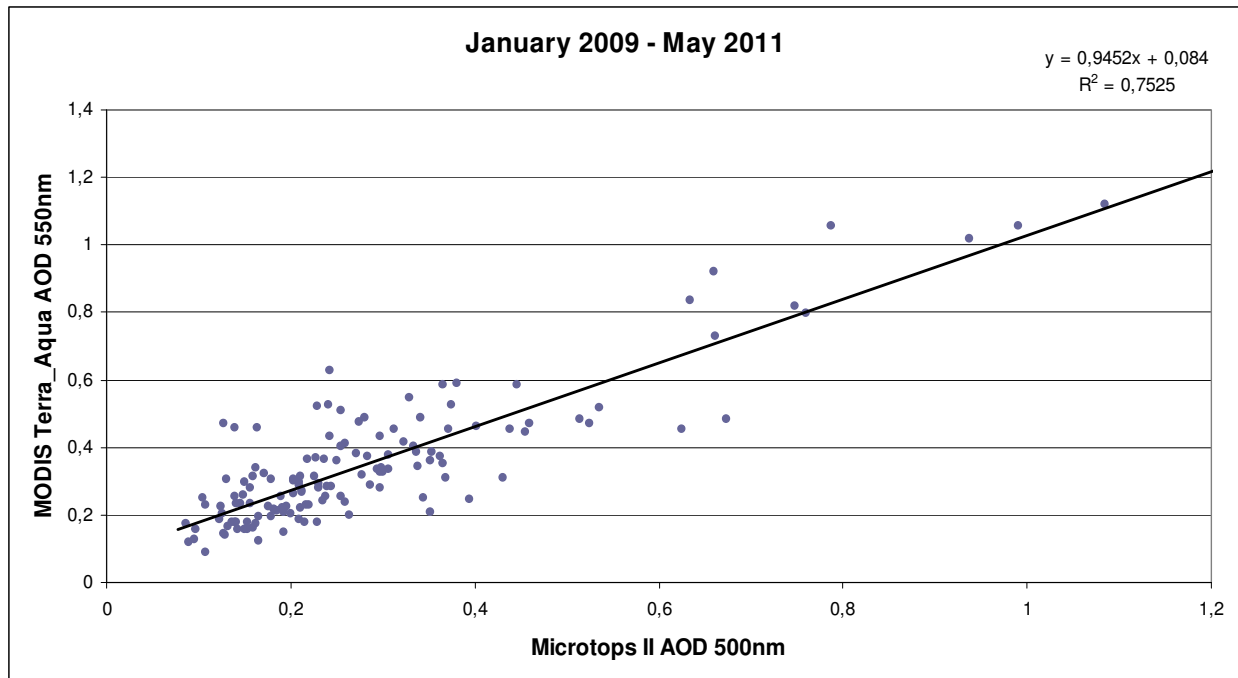


Fig. 18. Correlation between MODIS AOD and Microtops AOD for Limassol, January 2009 - May 2011 (Nisantzi et al., 2011).

In order to develop a regression model between MODIS data and PM₁₀, Nisantzi et al. (2011) attempted several correlations between PM₁₀ and AOT sun-photometer prior to the MODIS correlation in order to be more accurate. Nisantzi et al. (2011) acquired PM₁₀ data (using the DUST TRAK -Figure 9) every 10 minutes and AOD measurements for the CIMEL sun photometer at the same time, with a possible deviation 5 minutes. The correlation is shown in fig.19.

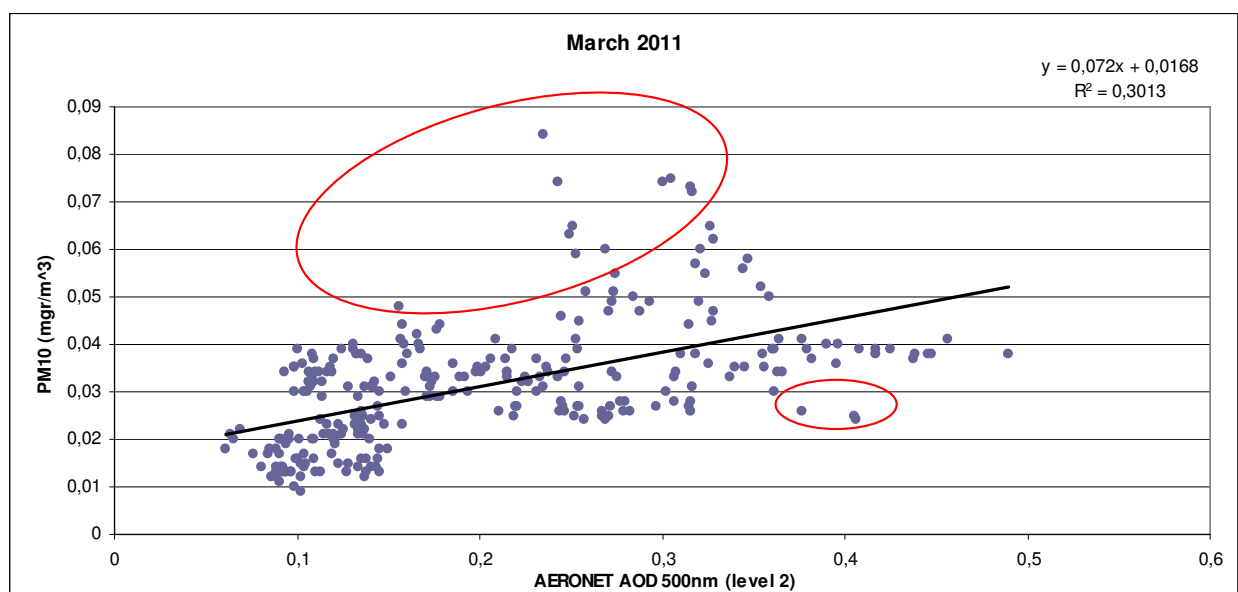


Fig. 19. Correlation between PM₁₀ and AERONET AOD for Limassol area, March 2011 (Nisantzi et al., 2011).

Nisantzi et al. (2011) considered the effect of dust in the field campaign measurements. By taking into consideration the measurements within the red cycles it was found that these measurements corresponded to days with dust layer above the ABL. Also examined the lidar measurements (see Figure 6) and by using backward trajectories for the three dust events (3/3/2011-5/3/2011, 16/3/2011-18/3/2011 and 28/3/2011-31/3/2011) occurred within this period. Nisantzi et al. (2010) excluded the data for these days and the correlation increased as shown in Fig. 20 (n=231, R=0.68). By excluding the measurements with aerosol layer above the ABL from both sun photometer and MODIS data, the correlation between the two variables PM₁₀ Vs. AOD (MODIS & Sun photometer) increases and the plots are shown in figures 21, 22.

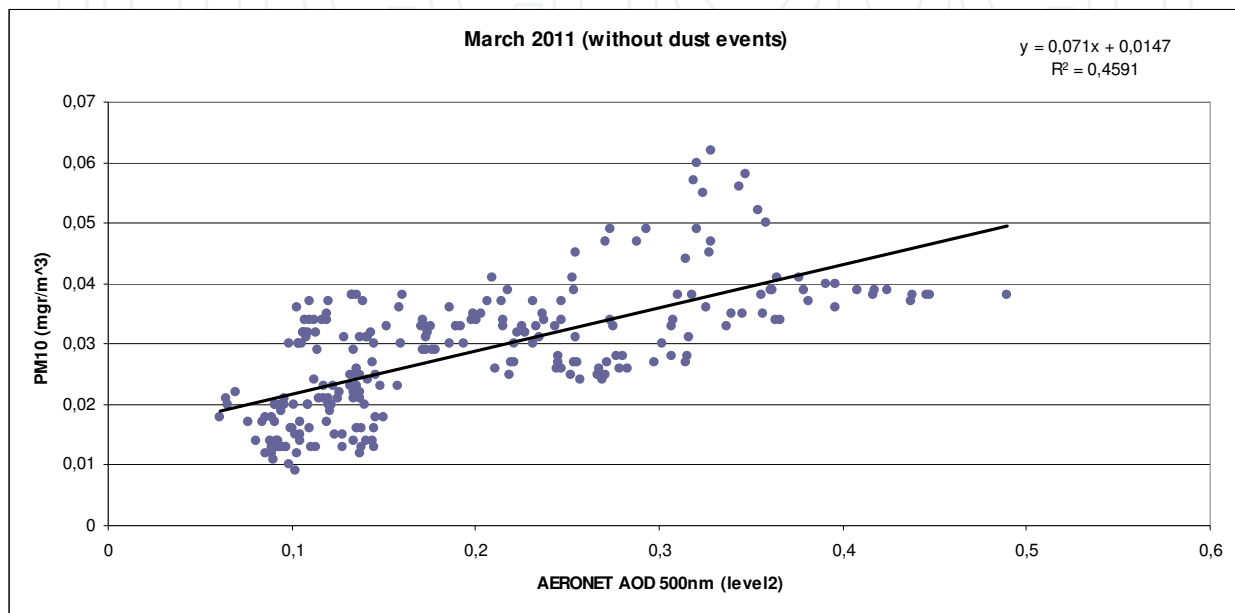


Fig. 20. Correlation between PM₁₀ and AERONET AOD (level 2) for Limassol area for March 2011 after excluding days with dust layers (Nisantzi et al., 2011).

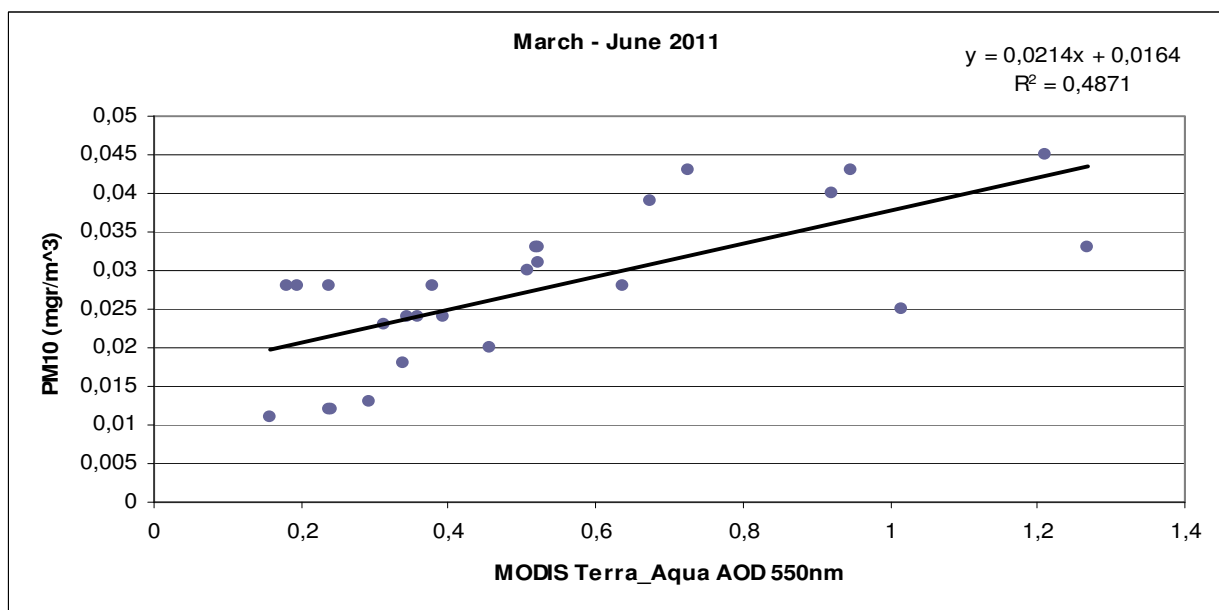


Fig. 21. Correlation between PM₁₀ and MODIS-derived AOD (Nisantzi et al., 2011).

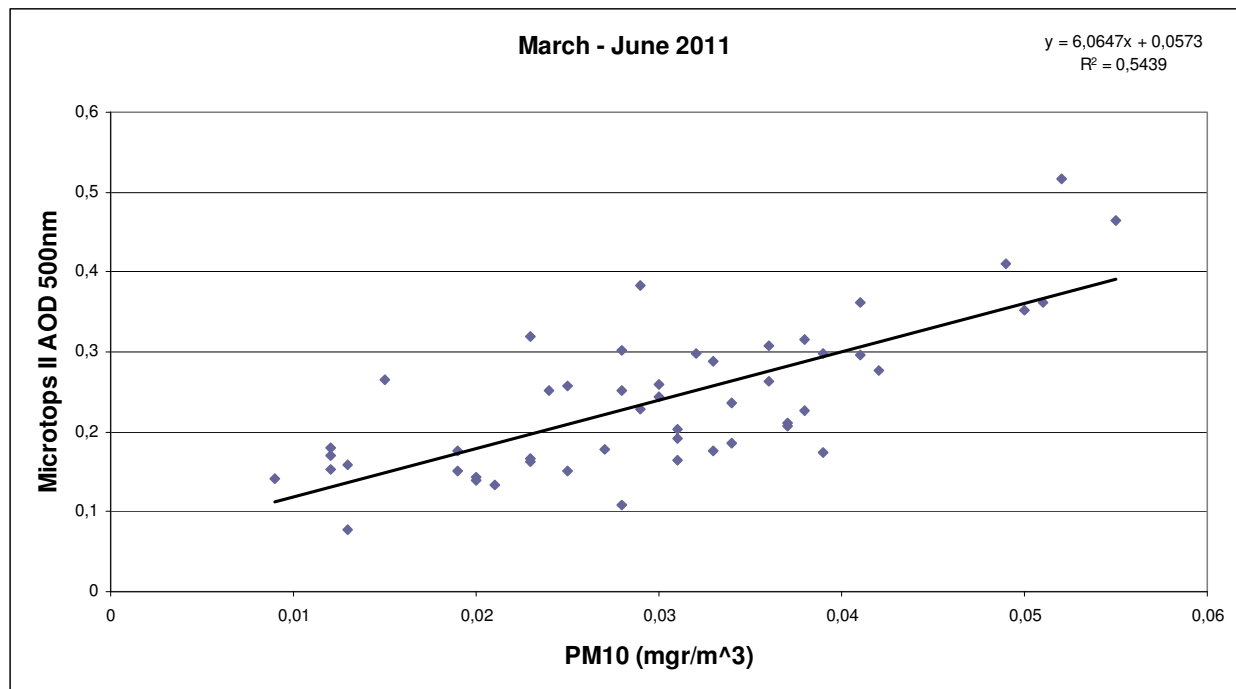


Fig. 22. Correlation between PM₁₀ and Microtops II-derived AOD (Nisantzi et al., 2011).

8. GIS

GIS has the advantage of the high power of analysing of spatial data and handling large spatial databases. Indeed, in air pollution there are a large amount of data that GIS can be used for their handling. Data that is used for air pollution studies is air pollutants, wind direction, wind speed, traffic flow, solar radiation, air temperature, mixing height etc. The integration of both GIS and remote sensing provides an deal efficient tool for the air pollution monitoring authorities (Zhou, 1995)

With GIS, remote sensing data can be integrated with other types of digital data, such as air pollution measures. Merging satellite remote sensing and GIS tools provides a quick and cost effective way to provide an improved qualitative assessment of pollution. GIS is a tool that can be used for assessing the air pollution through the use of AOT values retrieved directly from satellite imagery or in-situ sun-photometers, from air pollution measurements including CO₂, CO, SO₂, PM₁₀ and other environmental data. The integration of the above information can be inserted into a GIS software which can monitor and map high risk areas resulting air pollution. By using the AOT values retrieved from satellite, a thematic map can be developed through the application of Kriging algorithm in order to indicate high-polluted areas. Based on the determined AOT over an area of interest, and through interpolation, thematic maps can be generated using colour themes showing the levels of the AOT and/or pollution. Such information can be used as a tool for decision-makers to address air quality and environmental issues more effectively. Figure 23 shows a typical example of air pollutants over Cyprus using a GIS.

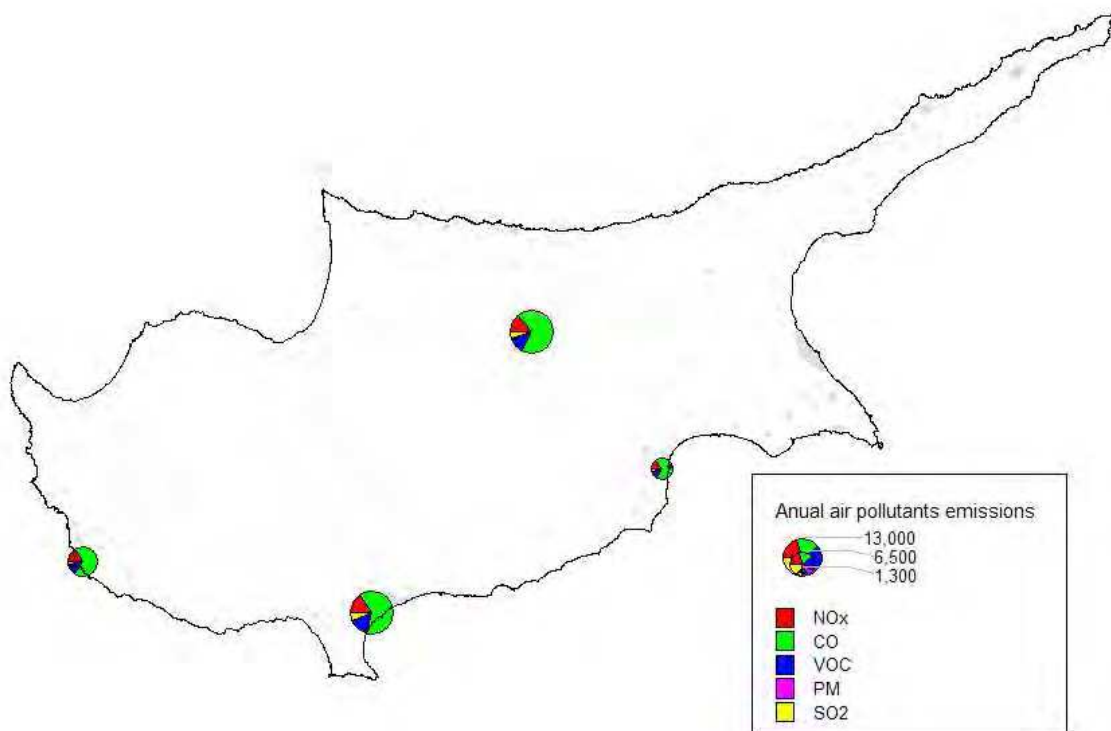


Fig. 23. GIS indicating air pollutant emissions in Cyprus.

Several studies showed the importance of using both GIS tools as well as satellite remotely sensed imagery to view and analyze the concentration of air pollutants and linkages with land cover and land use (Hashim and Sultan, 2010; Weng et al; 2004; 2006).

8.1 Case study

After determining the AOT using both MODIS (direct method) and Landsat TM/ETM imagery (indirect method), AOT thresholds were established based on PM10 measurements acquired over studies shown in section 7.1 and 7.2. Using the developed regression models shown in study area 7.2, thresholds of AOT values were obtained using the relevant limit, which is $50\mu\text{g}/\text{m}^3$ as prescribed by the European Union. Then, a GIS map was developed using the Kriging algorithm to identify areas with PM10 measurements above the acceptable threshold in order to monitor and map high risk areas due to air pollution (figure 24) by blending together satellite imagery and GIS. The GIS was conducted by dividing the area of interest using grid cells. The study found that by using the AOT values from MODIS or Landsat, a GIS map can be produced which can show high-polluted areas as shown in Figure 24. Themistocleous (2010) developed the fast atmospheric correction algorithm and the simplified image based AOT retrieval based on RT equation for GIS modeling which was used to create a thematic map of AOT values over Limassol.

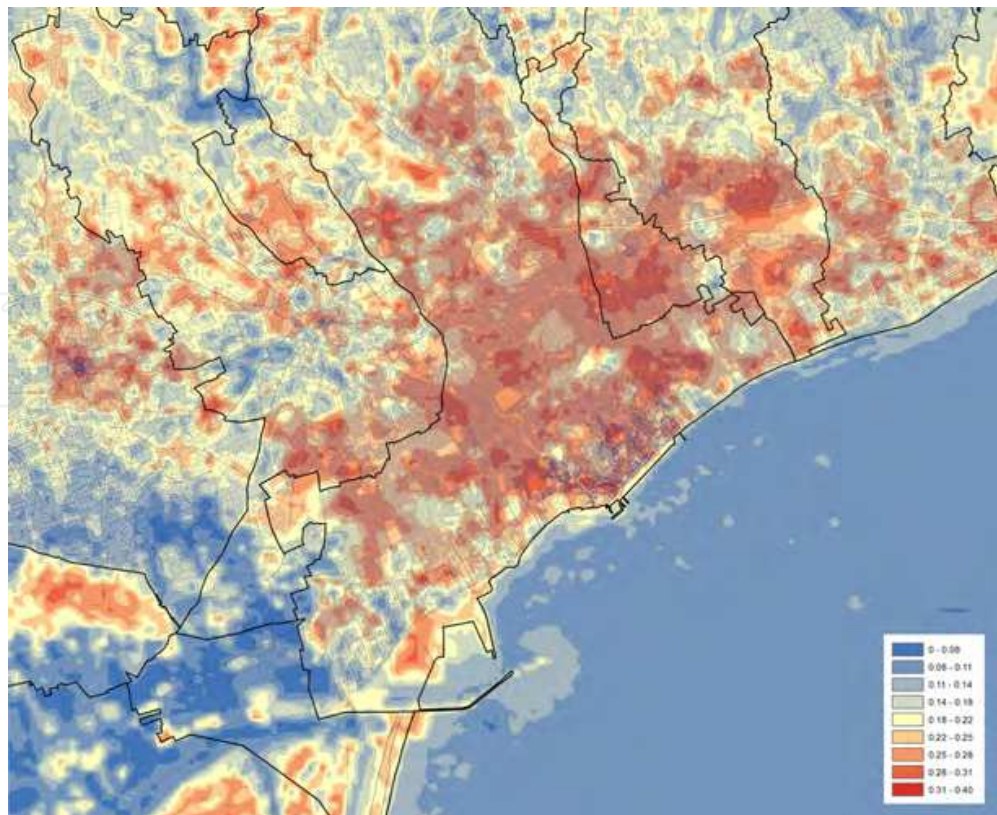


Fig. 24. GIS Thematic map using Krigging algorithm to display AOT levels in the Limassol area.

9. Conclusion

Earth observations made by satellite sensors are likely to be a valuable tool for monitoring and mapping air pollution due to their major benefit of providing complete and synoptic views of large areas in one snap-shot. Blending together GIS and remote sensing, AOT values can be derived over a large area of interest systematically. GIS is used also to map air pollutants based on ground and satellite-derived AOT values.

10. Acknowledgment

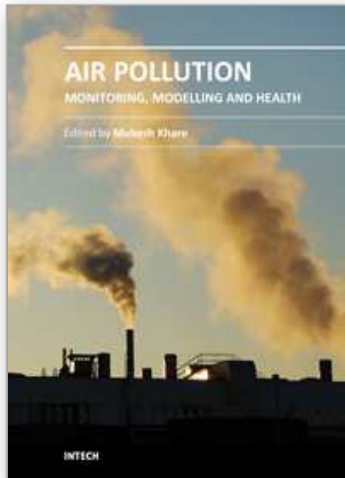
The authors acknowledge the Cyprus University of Technology (Research Committee) for their funding ('MONITORING' internal funded project) & research activity funds and the Cyprus Research Promotion Foundation for their funding ('AIRSPACE' research project). Special thanks are given to the Remote Sensing Lab of the Cyprus University of Technology.

11. References

- Chu, D. A., Kaufman, Y. J., Ichoku, C., Remer, L. A., Tanré, D., Holben, B. N. (2002). *Validation of MODIS aerosol optical depth retrieval over land*, *Geophys. Res. Lett.*, 29(12), pp. 8007.
- Hashim B. and Sultan A. (2010) Using remote sensing data and GIS to evaluate air pollution and their relationship with land cover and land use in Baghdad City, *Earth Sciences* 2 (2010) // 120-124

- Hadjimitsis, D.G. (2009a). *Aerosol Optical Thickness (AOT) retrieval over land using satellite image-based algorithm*, *Air Quality, Atmosphere & Health- An International Journal*, 2 (2), pp. 89-97 DOI 10.1007/s11869-009-0036-0
- Hadjimitsis, D.G. (2009b) *Description of a new method for retrieving the aerosol optical thickness from satellite remotely sensed imagery using the maximum contrast value principle and the darkest pixel approach*, *Transactions in GIS Journal* 12 (5), 633 – 644.
- Hadjimitsis, D.G., Clayton, C.R.I (2009). *Determination of aerosol optical thickness through the derivation of an atmospheric correction for short-wavelength Landsat TM and ASTER image data: an application to areas located in the vicinity of airports at UK and Cyprus*. *Applied Geomatics Journal*. 1, pp. 31--40
- Hadjimitsis, D.G., Retalis A., Clayton, C.R.I. (2002). *The assessment of atmospheric pollution using satellite remote sensing technology in large cities in the vicinity of airports*. *Water, Air & Soil Pollution: Focus, An International Journal of Environmental Pollution* 2, pp. 631 – 640.
- Hadjimitsis, D.G., Clayton C.R.I., & Hope V.S. (2004). *An assessment of the effectiveness of atmospheric correction algorithms through the remote sensing of some reservoirs*, *International Journal of Remote Sensing*, Volume 25, 18, 3651-3674. DOI: 10.1080/01431160310001647993
- Hadjimitsis, D. G., Nisantzi, A., Themistocleous, K., Matsas, A., Trigkas, V. P. (2010). *Satellite remote sensing, GIS and sun-photometers for monitoring PM10 in Cyprus: issues on public health*, *Proc. SPIE 7826, 78262C* (2010); doi:10.1117/12.865120
- Holben, B.N., Eck T.F., Slutsker I., Tame D., Buis J.P., Setzer A., Vermote, E., Reagan, J.A., Kaufman, Y., Nakajima, T., Lavenu F., Jankowiak, I., Smimov, A. (1998). *AERONET – A federated instrument network and data archive for aerosol characterization*, *Rem. Sens. Environ.* 66, pp. 1 – 16.
- Kaufman, Y.J., Fraser, R.S., Ferrare, R.A. (1990) *Satellite measurements of large-scale air pollution: methods*, *Journal of Geophysics Research* 95, pp. 9895 – 9909.
- King, M.D., Kaufman, Y.J., Tanré, D., Nakajima, T. (1999). *Remote Sensing of Tropospheric Aerosols from Space: Past, Present, and Future*, *Bulletin of the American Meteorological Society* 80, pp. 2229--2259
- Knobelspiessea, K. D., Pietrasa, C., Fargiona, S. G., Wanga, M., Frouine, R., Millerf, M. A., Subramaniang, A., Balchh, W. M. (2004). *Maritime aerosol optical thickness measured by handheld sun photometers*, *Remote Sensing of Environment* 93, pp.87 – 106.
- Lee, H. J., Liu, Y., Coull, B. A., Schwartz, J., and Koutrakis, P. (2011). *A novel calibration approach of MODIS AOD data to predict PM2.5 concentrations*, *Atmos. Chem. Phys.*, 11, 7991-8002, doi:10.5194/acp-11-7991-2011, 2011.
- Nisantzi A., Hadjimitsis D.G., Aexakis D. (2011) *Estimating the relationship between aerosol optical thickness and PM10 using lidar and meteorological data in Limassol, Cyprus*, *SPIE Remote Sensing 2011, Prague Sept.2011* (in press)
- Raju, P.L.N. (2003). *Fundamentals of Geographical Informatin Systems. Proceedings of Satellite Remote Sensing and GIS Applications in Agricultural Meteorology 7-11 July 2003, Dehra Dun, India*, p.p. 103-120.
- Retalis, A., Cartalis, C., Athanasiou, E. (1999) *Assessment of the distribution of aerosols in the area of Athens with the use of Landsat TM*. *International Journal of remote Sensing* 20, pp. 939 – 945.
- Retalis, A.: *Study of atmospheric pollution in Large Cities with the use of satellite observations: development of an Atmospheric correction Algorithm Applied to*

- Polluted Urban Areas, Phd Thesis, Department of Applied Physics, University of Athens (1998).
- Retalis, A.; Hadjimitsis, D.G. Chrysoulakis, N.; Michaelides, S.; Clayton, C.R.I. (2010). *Comparison between visibility measurements obtained from satellites and ground*, Natural Hazards and Earth System Sciences Journal, 10 (3) p.p. 421-428 (2010) doi:10.5194/nhess-10-421-2010
- Sifakis, N., Deschamps, P.Y. (1992) *Mapping of air pollution using SPOT satellite data*. Photogrammetric Engineering and Remote Sensing, 58, 1433 – 1437.
- Sivakumar, V., Tesfaye, M., Alemu, W., Moema, D., Sharma, A., Bollig, C., Mengistu, G. (2006) *CSIR South Africa mobile LIDAR- First scientific results: comparison with satellite, sun-photometer and model simulations*, South Africa Journal of Science 105, pp. 449 – 455.
- Schott, J.R. (2007). *Remote Sensing: the image chain approach*. Oxford, UK. Oxford University Press.
- Tang, J., Xue, Y., Yu, T., Guan, Y. (2004) *Aerosol optical thickness determination by exploiting the synergy of Terra and Aqua MODIS*. Remote Sensing of Environment 94, pp. 327 – 334.
- Themistocleous K., Nisantzi A., Hadjimitsis D., Retalis A., Paronis D., Michaelides S., Chrysoulakis N., Agapiou A., Giorgousis G. and Perdikou S. (2010) *Monitoring Air Pollution in the Vicinity of Cultural Heritage Sites in Cyprus Using Remote Sensing Techniques*, Digital Heritage, Lecture Notes in Computer Science, 2010, Vol. 6436/2010, 536-547, DOI: 10.1007/978-3-642-16873-4_44. M. Ioannides (Ed.): EuroMed 2010, LNCS 6436, pp. 536–547, 2010, © Springer-Verlag Berlin Heidelberg 2010.
- Tsanev, V. I., Mather, T. A. (2008) *Microtops Inverse Software package for retrieving aerosol columnar size distributions using Microtops II data*, Users Manual.
- Tulloch, M., Li, J. (2004) *Applications of Satellite Remote Sensing to Urban Air-Quality Monitoring: Status and Potential Solutions to Canada*, Environmental Informatics Archives, 2, pp. 846 – 854.
- Wald, L., Basly, L., Balleynaud, J.M. (1999) *Satellite data for the air pollution mapping*. In: 18th EARSeL symposium on operational sensing for sustainable development, pp.133--139 Enschede, Netherlands.
- Wang, J., Christopher, S. A. (2003) *Intercomparison between satellite derived aerosol optical thickness and PM_{2.5} mass: Implications for air quality studies*, Geophys. Res. Lett., 30 (21), pp. 2095 (2003).
http://daac.gsfc.nasa.gov/data-holdings/PIP/aerosol_optical_thickness_or_depth.shtml
- Zhou, Q. (1995). The integration of GIS and remote sensing for land resource and environment management. *Proceedings of United Nation ESCAP Workshop on Remote Sensing and GIS for Land and Marine Resources and Environmental Management*, 13-17 February, 1995. Suva, Fiji, p.p. 43-55.
- Weng, Q., Lub, D., Schubring, J. (2004) *Estimation of land surface temperature - vegetation abundance relationship for urban heat island studies*, Remote Sensing of Environment, v.89 (4), p. 467-483,
- Weng, Q., Yang, S (2006) *Urban air pollution patterns, land use and thermal landscape: an examination of the linkage using GIS Environmental Monitoring and Assessment*, v.117 (4), p.463-489.



Air Pollution - Monitoring, Modelling and Health

Edited by Dr. Mukesh Khare

ISBN 978-953-51-0424-7

Hard cover, 386 pages

Publisher InTech

Published online 23, March, 2012

Published in print edition March, 2012

Air pollution has always been a trans-boundary environmental problem and a matter of global concern for past many years. High concentrations of air pollutants due to numerous anthropogenic activities influence the air quality. There are many books on this subject, but the one in front of you will probably help in filling the gaps existing in the area of air quality monitoring, modelling, exposure, health and control, and can be of great help to graduate students professionals and researchers. The book is divided in two volumes dealing with various monitoring techniques of air pollutants, their predictions and control. It also contains case studies describing the exposure and health implications of air pollutants on living biota in different countries across the globe.

How to reference

In order to correctly reference this scholarly work, feel free to copy and paste the following:

Diofantos G. Hadjimitsis, Kyriacos Themistocleous and Argyro Nisantzi (2012). Air Pollution Monitoring Using Earth Observation & GIS, Air Pollution - Monitoring, Modelling and Health, Dr. Mukesh Khare (Ed.), ISBN: 978-953-51-0424-7, InTech, Available from: <http://www.intechopen.com/books/air-pollution-monitoring-modelling-and-health/air-pollution-monitoring-using-earth-observation-gis>

INTECH
open science | open minds

InTech Europe

University Campus STeP Ri
Slavka Krautzeka 83/A
51000 Rijeka, Croatia
Phone: +385 (51) 770 447
Fax: +385 (51) 686 166
www.intechopen.com

InTech China

Unit 405, Office Block, Hotel Equatorial Shanghai
No.65, Yan An Road (West), Shanghai, 200040, China
中国上海市延安西路65号上海国际贵都大饭店办公楼405单元
Phone: +86-21-62489820
Fax: +86-21-62489821

© 2012 The Author(s). Licensee IntechOpen. This is an open access article distributed under the terms of the [Creative Commons Attribution 3.0 License](#), which permits unrestricted use, distribution, and reproduction in any medium, provided the original work is properly cited.

IntechOpen

IntechOpen